

# Influences of the Dynamic Strain Aging on the J-R Fracture Characteristics of the Ferritic Steels for Reactor Coolant Piping System

Kook-Chul Kim, Jeong-Tae Kim, Jin-Ik Suk, Un-Hak Sung and Hee-Kyung Kwon

Doosan Heavy Industries & Construction Co., Ltd., Korea

## ABSTRACT

The leak-before-break (LBB) design of piping system for nuclear power plant has been based on the premise that the leakage due to the through-wall crack can be detected using leak detection systems before a catastrophic break. The piping materials are required excellent J-R fracture characteristics. However, ferritic steels for reactor coolant piping system have operated in a range of dynamic strain aging (DSA) temperature, so that the fracture resistance could be reduced by the influence of DSA under dynamic loading. Therefore, in order to apply the LBB design concept in piping system under seismic loading, both static and dynamic J-R characteristics must be evaluated.

The materials used in this study are SA 516 Gr.70 for elbow pipe, SA 508 Cl.1a for main pipe and welding joints of main pipe. The crack extension during dynamic and static J-R tests were measured by the direct current potential drop and the compliance method, respectively. This paper describes the influences of dynamic strain aging on the J-R fracture characteristics with loading rate of the pipe materials and their welding joints.

## INTRODUCTION

The design of primary and secondary piping in Korean Standard Nuclear Power Plants is applied on the Leak-Before-Break (LBB) concept. The piping materials applied to LBB concept should have an excellent fracture toughness in order to prevent unstable fracture piping due to the large through-wall crack. Therefore, to verify the integrity of piping materials, it is required to perform on tensile test and fracture toughness test (J-R Test). The tensile test should be carried out for determination of the detectable leakage crack length and elastic plastic FEM analysis for piping with the through-wall crack. The fracture toughness (J-R test) should be carried out for the crack stability evaluation of piping under normal operation loading loads and safe shutdown earthquake loads.

In the case of fracture toughness tests, static and dynamic J-R tests were performed for reactor coolant piping system made of carbon steel. The dynamic J-R test is required to prevent instability fracture due to a sudden drop of fracture toughness under seismic loading. In this paper, as a research for applying LBB concept to the reactor coolant piping system of Ulchin 5 and 6, we would study on the influences of dynamic strain aging on the J-R fracture characteristics with loading rate of the pipe materials and their welding joints.

## EXPERIMENTAL PROCEDURES

Static J-R tests were performed by unloading compliance method in accordance with ASTM E813-89[1] and ASTM E1152-87.[2] Dynamic J-R tests were performed by direct current potential drop method (DCPD) in accordance with ASTM E1737-96 A5[3] due to the rapid loading speed. Three valid tests at design temperature 316°C were performed for each selected heat of base metal and weld metal. In the case of dynamic J-R test, additional valid test at hot standby temperature 177°C and room temperature was performed to investigate temperature dependency.

**Table 1. Fracture toughness test number**

Item			Material	Dynamic J-R Test			Static J-R Test
				25°C	177°C	316°C	316°C
Base Metal	RCS Main Loop Piping	Hot Leg	SA508 Gr. 1a	1	1	3	3
		Cold Leg	SA508 Gr. 1a	1	1	3	3
		Elbow	SA516 Gr. 70	1	1	3	3
Weld Metal	Main Loop Piping Segments		E7016 (SMAW-Manual)	1	1	3	3
			US-40N7PFH-55SN (SAW-Automatic)	1	1	3	3
Total				25			15

## Testing Apparatuses

The machine used for this test is servo-hydraulic universal test machine with loading capacity of 25 ton. Test apparatus was calibrated in accordance with ASTM E4 and confirmed within  $\pm 1\%$  of the working range. The chamber for high temperature test was used. The extensometer for high temperature was used for measuring extended length of tensile specimen. In J-R test, load line displacement was measured by using the crack opening displacement gage (Capecitec Model P-COD Gage) for high temperature.

## Materials and Specimens

The Ulchin 5 and 6 plant design employs a two-loop reactor coolant piping system, each loop containing a steam generator and two reactor coolant pumps as shown in Fig. 1. Each hot leg is a 42 inch Inner Diameter pipe of SA508 Cl.1a material with 3- $\frac{1}{2}$  inch nominal thickness. The cold leg is 30 inch Inner Diameter pipes of SA508 Cl.1a material with 3 inch nominal thickness walls. The elbow material is SA 516 Gr.70. The straight pipe and elbow are welded by SAW automatic welding and SMAW manual welding. The specimens for elbow base metal were taken for plate before hot-rolling. Weld deposits for weld metal test specimens were prepared using the same welding procedure and the same heat of weld material used in the production weld. The detailed welding conditions are shown at Table. 2. Table 3 indicates chemical compositions for each material.

Tensile tests were used on round specimens with diameter of 6.25mm with orientation in L direction, and fracture toughness tests were used on 1 inch compact tension specimen with orientation in L-C direction. In the case of dynamic J-R test specimens, current input wires were mechanically fastened to the both side of the specimen by screw, and voltage measurement wires with diameter of 0.7mm are welded by spot welding as shown in Fig. 2.

**Table 2. Welding Procedures**

Process	Filler metal		PWHT Temp.	Amp. Range	Volt. Range	Travel Speed (cm/min)
	AWS No.	Size(mm)				
SMAW (Manual Welding)	E7016	$\Phi$ 3.2	615 $\pm$ 20°C	90 ~ 130	20 ~ 28	6 ~ 15
		$\Phi$ 4.0	615 $\pm$ 20°C	130 ~ 180	20 ~ 28	8 ~ 18
		$\Phi$ 5.0	615 $\pm$ 20°C	180 ~ 240	20 ~ 35	15 ~ 22
150 ~ 190	20 ~ 30			9 ~ 13		
SAW (Automatic Welding)	US-40N7PFH-55SN	$\Phi$ 2.4	615 $\pm$ 20°C	300 ~ 400	27 ~ 32	20 ~ 35
		$\Phi$ 4.0	615 $\pm$ 20°C	500 ~ 600	28 ~ 32	30 ~ 40

**Table 3. Chemical Composition (% wt)**

Pipe	C	Si	Mn	P	S	Cu	Mo	V	Ni	Cr	Al
Hot Leg	0.22	0.206	1.18	0.010	0.0014	0.10	0.056		0.23	0.096	0.032
Cold Leg	0.199	0.216	1.15	0.010	0.0024	0.139	0.038		0.219	0.106	0.020
Elbow	0.17	0.31	1.13	0.008	0.001	0.18	0.10	0.025	0.34	0.01	
SMAW Weld	0.065	0.49	1.04	0.019	0.008	0.04	0.05	0.03			
SAW Weld	0.08	0.26	1.59	0.009	0.002	0.02	0.51	<0.01			

## Tensile Test

Tensile tests were performed in accordance with ASTM E21.[4] Yield strength was determined by 0.2% offset method. From load-displacement curve obtained through test, true stress-true strain curve was obtained, and then material constant  $\alpha$ , n was obtained by fitting the true stress-true strain data with the normalized Ramberg-Osgood relation as follow.

$$\frac{\epsilon}{\epsilon_0} = \frac{\sigma}{\sigma_0} + \alpha \left( \frac{\sigma}{\sigma_0} \right)^n \quad (1)$$

where,  $\epsilon_0$ : the strain at yield point,  $\sigma_0$ : true yield strength,  $\alpha$ : Ramberg-Osgood material constant, n: strain hardening exponent.

## Static J-R Test

Static J-R tests were performed by unloading compliance method in accordance with ASTM E813-89 and ASTM E1152-87. At first, the compact tension specimens were precracked by cyclically loading until crack length was about 0.6W. Then, side groove was performed to go straight of crack, where the depth of side groove is 20% of specimen thickness. In test, the specimen was held at test temperature in chamber for 1 hour to uniform heat distribution over specimen, and was tested by unloading compliance method. The range of unload/reload for crack extension measurement was 30% of the current load. After the test, the specimen was broken at subzero temperature to compare measured crack extension length with calculated

crack extension length.

### Dynamic J-R Test

The specimen crack length of dynamic J-R test was measured by direct current potential drop method (DCPD). Test speed was determined by natural frequency method proposed at Battelle.

$$V_{LL} = 4 \times \text{natural frequency}(\text{mode } 1) \times D_i \quad (2)$$

where,  $D_i$  is load line displacement at crack initiation of static J-R test. The natural frequency was 10Hz, and test speed of 1,000mm/min was determined for all materials.

The schematic drawing of dynamic J-R test is shown in Fig. 3. The specimen was isolated from load frame by inserting Bakelite plates which have strength and isolation between the test jig and the machine frame, and 100-Ampere constant current was supplied to the specimen using power supply in order to measure crack growth length during the test. For high-speed data acquisition, HP3852A DAS System was used. The modules are HP44704A High Speed Voltmeter and HP44711A High Speed FET Multiplexer. Using the acquisition system, the variation of load, COD value and output voltage were acquired digitally to computer during test.

Test procedure is as follows; first, the specimen was precracked by cyclically loading and side-grooved. After attaching current input wires and voltage measurement wires, the specimen was installed on testing machine. At high temperature test, the specimen was held during 1 hour in the chamber at test temperature. Then, output voltage was measured with the current off to measure basis voltage. In the case of high temperature test, the basis voltage was higher than one at room temperature. Therefore, to compensate the thermal effect, the final voltage was obtained by subtracting voltage measurements taken with the current off from the total measured voltage. Dynamic J-R tests were performed on the specimen at 1,000mm/min under stroke control with the current on. In analysis, after crack initiation point was obtained from COD values versus output voltage curve, the variation of crack length was calculated from Johnson's equation [6] for all data after crack initiation point.

$$\frac{a}{W} = \frac{2}{P} \cos^{-1} \left[ \cosh \left( \frac{P}{2W} \right) / \cosh \left[ \left( \frac{U}{U_0} \right) \cosh^{-1} \left[ \frac{\cosh \left( \frac{P}{2W} \right)}{\cos \left( \frac{P_0}{2W} \right)} \right] \right] \right] \quad (3)$$

where,

- U = electric potential signal,
- $U_0$  = initial electric potential signal, (= UB, In this case)
- a = crack length
- $a_0$  = initial crack length
- W = specimen width, and
- 2y = the spacing of the potential probes.

To confirm accuracy of the test, calculated crack length was compared with measured crack length from broken specimen.

## TEST RESULTS

### Static J-R Test

At the early research period for J-R experiment of those materials, negative crack behaviors and large data scatter had been shown due to the high ductility. We realized from several tests that one of the reasons was needless contact between the specimen and the grip. Static J-R test was performed until COD displacement was 10 mm for obtaining J-R curve of high energy piping materials. The loading pin became rotated on the clevis holes due to the large travel of the COD gage. In order to provide rolling contact sufficiently between the loading pin and the clevis holes, these holes should be provided with larger flats than 0.07W recommended at ASTM E1820 on the loading surfaces due to more rolling movement of pin. (Our flat length: 8.5mm, 0.167W) Moreover, another reasons for data scatter was contact between a side of specimen and a side of grip. Therefore, The clevis grip was machined as shown Fig. 4 in order to have gap sufficiently between the specimen and the clevis grip. As a result, we could valid J-R curves for high energy piping materials.

Fig. 5 shows static J-R curves for reactor coolant piping. For elbow base metal (SA516 Gr.70 steel) and SMAW manual welding metal, excellent static J-R properties are shown. The other side, J-R curves for SAW automatic welding metal are lowest among 5 materials. In comparison between hot leg pipe and cold leg pipe, The J-R curves of cold leg pipe are slightly higher than those of hot leg pipe. The reason can be found from forging effect.

All materials were not satisfied on size condition as valid  $J_{IC}$  value due to the high  $J_Q$  values. Meanwhile, when J-T<sub>R</sub> curve is obtained from J-R curve, the condition for satisfying J-controlled crack growth is as following equation.

$$w = \frac{dJ}{da} \cdot \frac{b}{J} > 1 \quad (4)$$

In this test result, crack extension length,  $0.3b_0$  is satisfied on the condition of  $\omega > 1$  for all materials, so we know that J-T<sub>R</sub> curve is valid until crack extension length is  $0.3b_0$ .

Table 4 shows tensile properties tested at 316°C and described at CMTR (Certified Material Test Report: Room Temperature).

**Table 4. Tensile Properties**

Pipe	Room Temp.		316°C	
	YS(MPa)	UTS(MPa)	YS(MPa)	UTS(MPa)
Hot Leg	352	526	233	498
Cold Leg	334	503	248	516
Elbow	334	494	234	474
SMAW Weld	434	529	337	467
SAW Weld	572	648	438	564

### Dynamic J-R Test

First, in order to confirm the test speed is 1,000mm/min, actual speed was measured from time versus COD displacement relationship. We could confirm the accuracy within 5 % of input speed. Fig.6 represents COD value versus output voltage curve for 5 materials. For all test materials appear pulse drop signals at initial loading region in Fig. 6. It is known that this phenomenon occurs due to the ferromagnetic effect. Namely, when the structure of ferromagnetic substance is changed rapidly, magnetic field is made in the material and electric potential difference is induced. Accordingly, it was difficult to measure crack length because a rapid loading voltage pulse superimposed on the d-c electric potential signal. In particular, it was difficult to find crack initiation point due to the pulse drop phenomenon. Also, we could not explain physical concept full enough for pulse behavior related to crack initiation.

Fig. 7 represents the variation of J-R curve according to temperature with respect to each material. It shows that J-R curve is decreased with the increasing test temperature. However, in the case of SAW automatic welding, brittle fracture occurred at room temperature. In general, the faster loading speed, the higher transition-temperature-region. The brittle fracture occurred because the specimen was tested at transition-temperature-region for SAW automatic welding metal at 1,000 mm/min. Fig. 8 shows dynamic J-R curves for reactor coolant piping. In order to compare dynamic J-R curve with static J-R curve easily,  $J_{0.1 \text{ inch}}$  values was obtained from J-R curves, and the variation of  $J_{0.1 \text{ inch}}$  value with loading rate at operating temperature, 316°C is shown in Fig. 9.  $J_{0.1 \text{ inch}}$  value at 1,000mm/min is lower than one at 1mm/min for elbow material (SA516 Gr.70 steel), but  $J_{0.1 \text{ inch}}$  value at 1,000mm/min is higher than one at 1mm/min for SAW automatic welding metal. For the other materials,  $J_{0.1 \text{ inch}}$  values between test speed of 1mm/min and 1,000mm/min are similar.

According to Kim's paper,[7] minimum crack initiation toughness,  $J_1$  is shown in dynamic strain aging (DSA) temperature region for given loading rate, and the temperature corresponding to the  $J_1$  value is higher with increasing loading rate. Based on this concept, we can explain the trend for loading rate shown in our experiment results. Namely, elbow material corresponds to type A material and SAW automatic welding metal corresponds to type B material in Fig. 10. From the fracture toughness with respect to loading rate, we know that elbow material (SA516 Gr.70 steel) and SAW automatic welding metal (US-40N7PFH-55SN) are susceptible to dynamic strain aging at the temperature range of 25°C ~ 316°C.

### CONCLUSION

For elbow base metal (SA516 Gr.70 steel) and SMAW manual welding metal, excellent static J-R properties are shown. The other side, J-R curves for SAW automatic welding metal are lowest among 5 materials.

$J_{0.1 \text{ inch}}$  value at 1,000mm/min is lower than one at 1mm/min for elbow material (SA516 Gr.70 steel), but  $J_{0.1 \text{ inch}}$  value at 1,000mm/min is higher than one at 1mm/min for SAW automatic welding metal. For the others materials,  $J_{0.1 \text{ inch}}$  values between test speed of 1mm/min and 1,000mm/min are similar.

### REFERENCES

1. ASTM E 813-89, "Standard Test Method for  $J_{IC}$ , A Measure of Fracture Toughness,"
2. ASTM E 1152-87, "Standard Test Method for Determining J-R Curves,"

3. ASTM E1737-96, "Standard Test Method for J-Integral Characterization of Fracture Toughness,"
4. ASTM E21, "Standard Test Methods for Elevated Temperature Tension Tests of Metallic Materials,"
5. Johnson, H.H., "Calibrating the Electric Potential Method for Studying Slow Crack Growth," *Materials Research & Standards*, pp442~445, September 1965.
6. ASTM E1820-99a, "Standard Test Method for Measurement of Fracture Toughness,"
7. Kim, J.W. and Kim, I.S., "Investigation of Dynamic Strain Aging on SA106-Gr.C Piping Steel," *Nuclear Engineering and Design*, Vol. 172, pp 49~59, 1997.
8. Lee, B.S. Yoon, J.H., Oh, Y.J., Kuk, I.H. and Hong, J.H., "Static and Dynamic J-R Fracture Characteristics of Ferritic Steels for RCS Piping," *SMIRT 15*, Vol. V pp. 297~302, 1999.
9. Mark P. Landow and Charles W. Marschall, "Experience in Using Direct Current Electric Potential to Monitor Crack Growth in Ductile Metals," *ASTM STP 1114*, pp. 163~177, 1991.

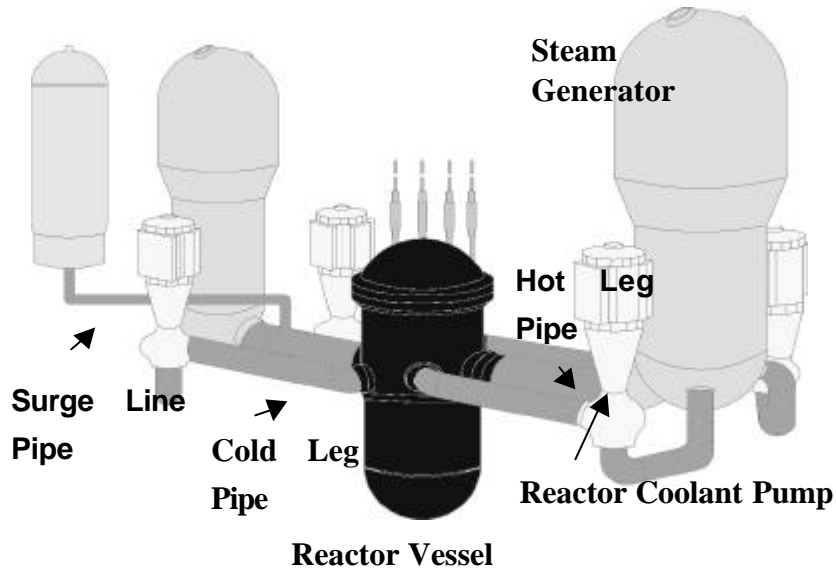


Fig. 1 Reactor Coolant Piping System

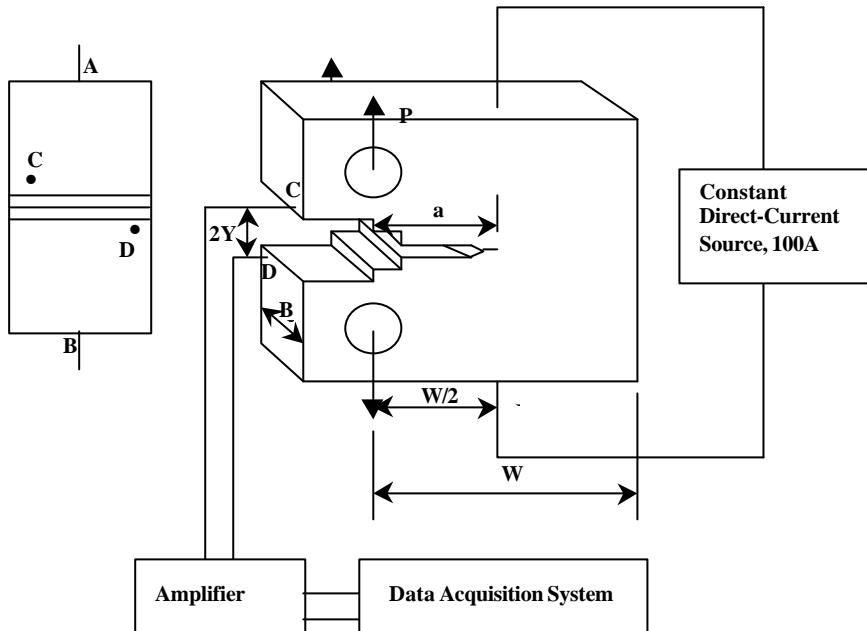
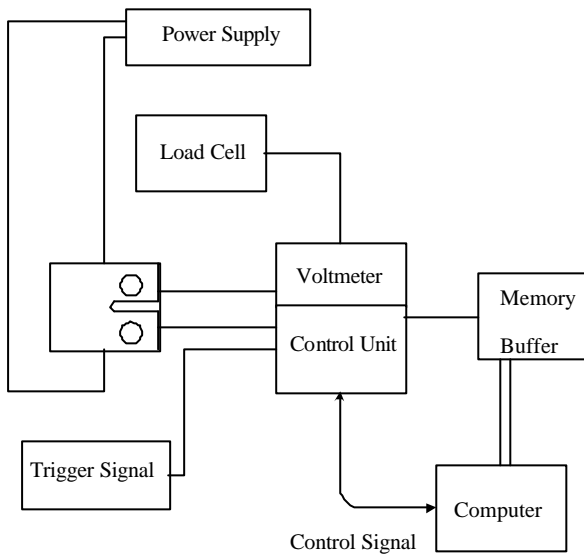
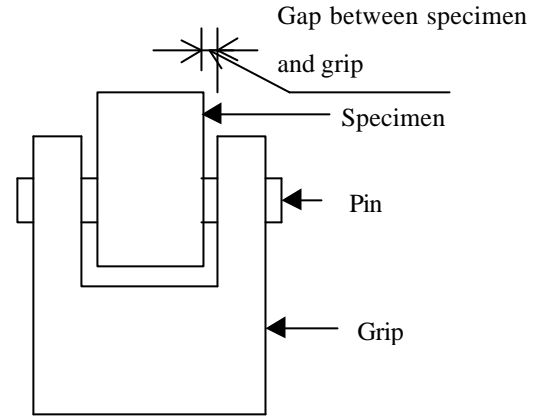


Fig. 2 The Specimen Geometry for Dynamic J-R Test



**Fig. 3 Data Acquisition System for Dynamic J-R Test**



**Fig. 4 The illustration for influence of the Gap between Grip and Specimen**

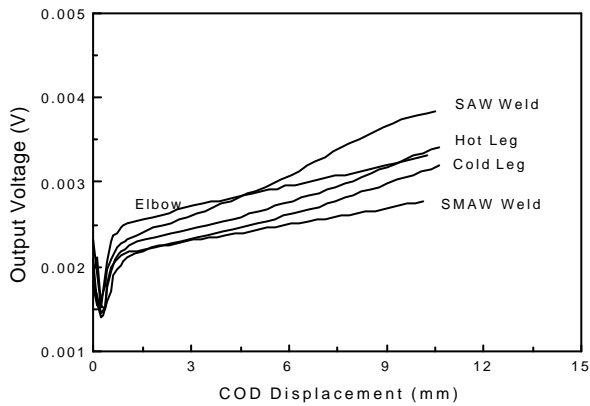


**Fig.5 COD Gage versus Output Voltage for Reactor Coolant Piping Materials**

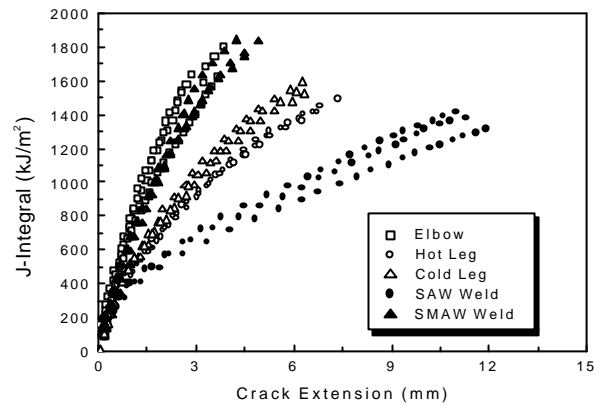
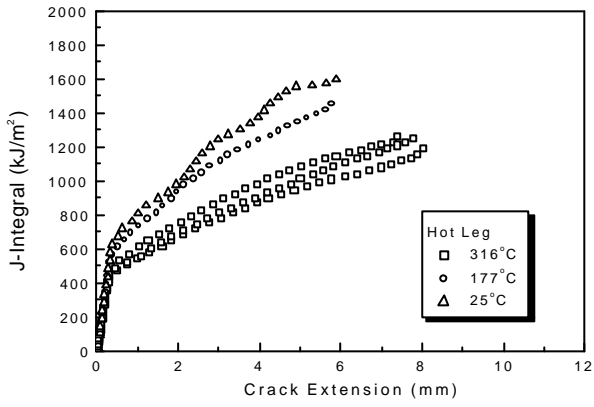
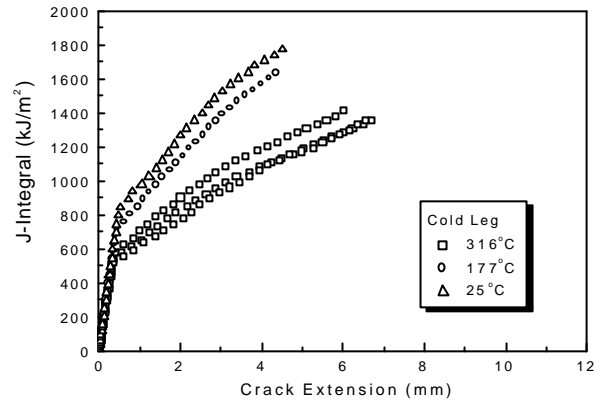


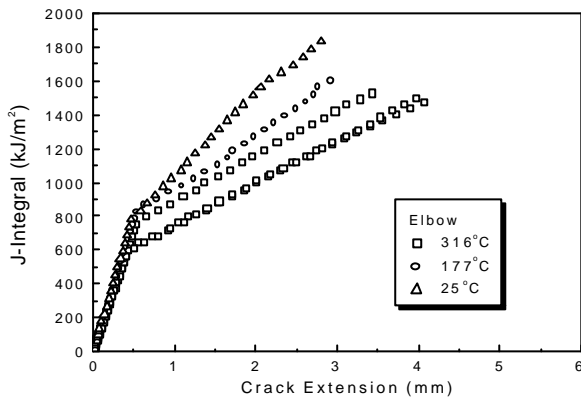
**Fig.6 Static J-R Curves at 316°C**



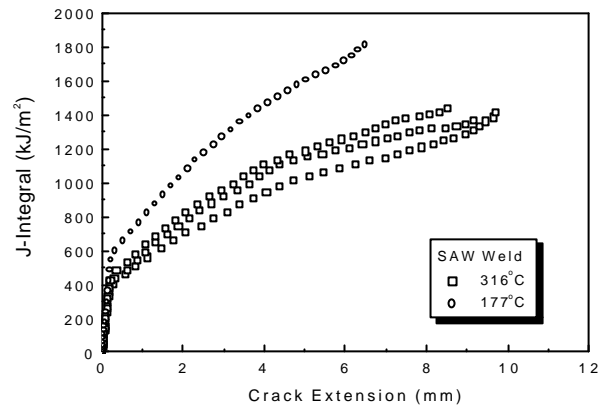
(a) Hot Leg Pipe (SA508 Cl.1a)



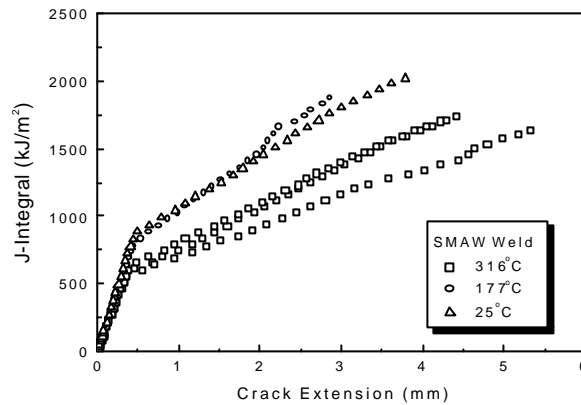
(b) Cold Leg Pipe (SA508 Cl.1a)



(c) Elbow (SA516 Gr. 70)



(d) SAW Weld



(e) SMAW Weld

Fig.7 Dependency of Dynamic J-R Curve on temperature

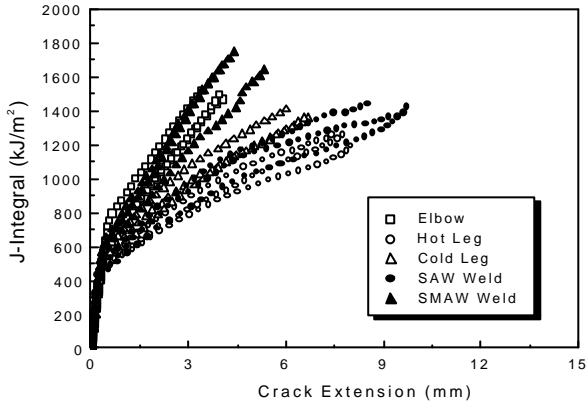


**Fig. 8 Dynamic J-R Curve at 316°C**

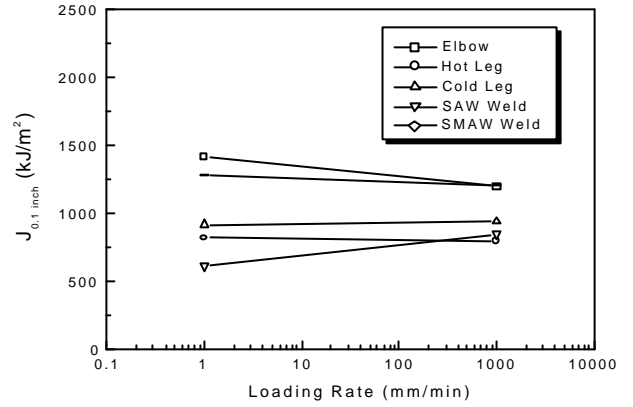


**Fig. 9 Dependence of J-R Fracture Toughness on the Loading Rate at 316°C**

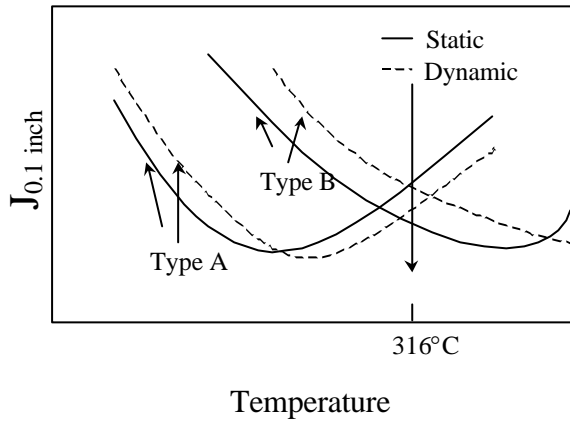


**Fig. 10 Dependency of Fracture Toughness on Temperature and Loading Rate in DSA Region**